



## ORIGINAL ARTICLE

# Structural characterization and immune-enhancing activity of a novel acid proteoglycan from Black soybean



Wuxia Zhang<sup>a,1</sup>, Yihua Hu<sup>a,1</sup>, Jiaqi He<sup>a</sup>, Yongpo Zhang<sup>a</sup>, Aiqin Yue<sup>b</sup>, Weijun Du<sup>b</sup>, Jinzhong Zhao<sup>a,\*</sup>, Peng Li<sup>a,\*</sup>

<sup>a</sup> Department of Basic Sciences, Shanxi Agricultural University, Taigu 030801, Shanxi, China

<sup>b</sup> College of Agriculture, Shanxi Agricultural University, Taigu 030801, Shanxi, China

Received 4 April 2022; accepted 5 June 2022

Available online 9 June 2022

## KEYWORDS

Black soybean;  
Proteoglycan;  
Immunoregulatory activity;  
Mannose receptor;  
NF-κB

**Abstract** Black soybean (*Glycine max* (L.) merr), as an edible seed of the leguminous plant, possesses a high amount of proteins and carbohydrates. However, few studies have been conducted on the protein-polysaccharide polymer (proteoglycan) in Black soybean. Here, we aim to characterize the proteoglycan in Black soybean. Firstly, a crude extract from Black soybean was obtained by water extraction and alcohol precipitation. Then, DEAE-52 cellulose and Sephadex G-100 column chromatography were used to isolate proteoglycans in the crude extract, and a novel proteoglycan named BBWPS2 was obtained. Moreover, the chemical analysis showed that BBWPS2 was a proteoglycan of  $2.02 \times 10^5$  Da, and composed of 7 kinds of monosaccharides and 16 kinds of amino acids.  $\beta$ -elimination reaction identified the carbohydrate chain was connected to peptide chain with *O*-glycosidic bonds. Finally, the immunomodulatory tests indicated that BBWPS2 can significantly promote the primary splenocyte proliferation and activate mouse peritoneal macrophages to produce TNF- $\alpha$ . Subsequent pathway studies revealed that BBWPS2 activated macrophages through the mannose receptor-mediated NF- $\kappa$ B/MAPK signaling pathway. Our work indicated that BBWPS2 from Black soybean could be explored as a promising natural immunopotentiator in food and pharmaceutical industries.

© 2022 Shanxi Agricultural university. Published by Elsevier B.V. on behalf of King Saud University. This is an open access article under the CC BY-NC-ND license (<http://creativecommons.org/licenses/by-nc-nd/4.0/>).

\* Corresponding authors.

E-mail addresses: [zhaojz@sxau.edu.cn](mailto:zhaojz@sxau.edu.cn) (J. Zhao), [lip@sxau.edu.cn](mailto:lip@sxau.edu.cn) (P. Li).

<sup>1</sup> These authors have contributed equally to this work.

Peer review under responsibility of King Saud University.



## 1. Introduction

Black soybean (*Glycine max* (L.) merr) was a plant of medicine food homology around East Asia, and rich in nutrients including protein, fatty acids, carbohydrates and vitamins (Jakab, 2016). Pharmacological studies have demonstrated that Black soybean possesses a variety of activities, including antioxidant activity, anti-diabetic activity (Hsieh-Lo and Castillo-Herrera, 2020), and anti-inflammatory activity

(Reverri et al., 2015) and immune-enhancing activity (Hayat et al., 2014). However, the chemical basis of these biological activities remains unknown. At present, there have been reports of confirmation, that soybean-fragmented proteoglycans may fight skin aging with an improvement in skin roughness (Barba et al., 2017). Proteoglycan isolated from *Phellinus linteus* activates murine B lymphocytes (Kim et al., 2003). Here, inspired by the fact that Black soybean contains plentiful proteins and polysaccharides, we consider that there may be protein-polysaccharide polymers in the Black soybean. This work aimed to isolate proteoglycans from Black soybean and identified their immune activities.

In this study, we intend to obtain proteoglycans from Black soybean by water extraction and alcohol precipitation, and column chromatography. Its structure was characterized by monosaccharide compositions, amino acid analysis,  $\beta$ -elimination reaction, Infrared spectra (IR) and Scanning Electron Microscopy (SEM) analysis. Then, the immunomodulatory function of BBWPS2 was examined at molecular and cellular levels.

## 2. Materials and methods

### 2.1. Materials and chemicals

Black soybean was produced in Taigu District, Shanxi Province, China. 1-phenyl-3-methyl-5-pyrazolone (PMP), bovine serum albumin, concanavalin A (ConA), lipopolysaccharide (LPS), mannose (Man), rhamnose (Rha), galacturonic acid (GalA), glucose (Glc), galactose (Gal), xylose (Xyl), arabinose (Ara) and fucose (Fuc) were purchased from Solarbio Science & Technology Co., Ltd. (Beijing, China). 3-(4-methylphenylsulfonyl)-2-propenenitrile (BAY 11-7082), Antibody NF- $\kappa$ B p65, FITC labeled Goat Anti-Rabbit IgG (H + L) and nuclear dye (DAPI) were purchased from Beyotime (Shanghai, China). All other chemicals were of analytical grade as available.

### 2.2. Cells

Mouse peritoneal macrophages (RAW264.7 cell line) were previously preserved in our laboratory. RAW264.7 cells were cultured with RPMI-1640 medium containing 10% fetal bovine serum. Primary spleen cells were obtained by lysis with Red Blood Cell Lysis Buffer, and cultured with RPMI-1640 medium containing 10% fetal bovine serum (Zhang et al., 2015a).

### 2.3. Extraction and purification of crude extract

Black soybean was peeled and pulverized. The dried Black soybean powder was pre-extracted with 95% ethanol to remove lipids. The residue powder was extracted 3 times with distilled water at 80 °C for 2 h. The supernatants were concentrated and collected with alcohol sedimentation. The precipitate was dissolved, dialyzed and lyophilized to obtain Black soybean crude extract named BBWP. BBWP was dissolved in distilled water and the mixture was centrifuged. The supernatant was loaded on DEAE-52 cellulose (5 × 50 cm, Cl<sup>-</sup> form), and eluted with distilled water and different concentrations of gradient NaCl solution (0.1, 0.2, 0.5 mol/L) at a flow rate of 0.5 mL/min consecutively. Finally, 0.2 mol/L NaCl elution components were collected and further purified on Sephadex

G-100 (Packing particle size: 40 ~ 120  $\mu$ m) and eluted with distilled water at a flow rate of 0.2 mL/min. Proteoglycan BBWPS2 was obtained. The isolation and purification steps are shown in Fig. 1.

### 2.4. Molecular weight determination

High-performance gel permeation chromatography (HPGPC) was used to determine the molecular weight (Zhang et al., 2015b). Series Dextrans (5.2, 11.6, 23.8, 48.6, 148, 668 kDa) and BBWPS2 were eluted by 3 mmol/L sodium acetate solution at 0.5 mL/min. The calibration curve of  $\log(M_w)$  vs. elution time (T) is  $\log(M_w) = -0.1719 T + 11.58$ .

### 2.5. Chemical and amino acid analysis

Neutral carbohydrate, protein and uronic acid content of BBWPS2 were determined by the phenol-sulphuric acid method (Zhang et al., 2020), Bradford's method (Hayes 2020) and *m*-hydroxydiphenyl-sulphuric acid method (Blumenkrantz and Asboe-Hansen 1973), respectively.

The amino acids of BBWPS2 were analyzed by an amino acid analyzer (S-433D, Sykam, Germany). Briefly, 2 mg BBWPS2 was completely hydrolyzed at 110 °C for 22 h with 6 mol/L HCl (solid-liquid ratio: 1:1) under the protection of nitrogen. The hydrolysate was filtered and adjusted to 10 mL. Then 1 mL filtrate was collected and dryness with the addition of 2 mL sample diluent water to redissolve. The solution was shaken, filtered with a 0.22  $\mu$ m filter membrane and determined by Amino Acid Analyzer (Zeng et al., 2015). The free amino acids of BBWPS2 monomers were analyzed by using acidic buffer as mobile phase, cation exchange resin as stationary phase and a dual-wavelength detector. The column temperature was 58°C. After reacting with ninhydrin, the derivatives of amino acids were detected by ultraviolet detection at 570 nm and 440 nm.

### 2.6. Monosaccharide composition analysis

Monosaccharide compositions were analyzed by high-performance liquid chromatography (HPLC) after precolumn-derivatization of the hydrolysate with PMP (Honda et al., 1989). Briefly, the BBWPS2 solution was hydrolyzed by TFA at 110 °C for 4 h and the sample was completely hydrolyzed. After the hydrolysate is cooled, the residual TFA is removed by rotary evaporation, and the hydrolysate is redissolved by distilled water. After fully mixing the polysaccharide hydrolysate or the standard solutions (Man, Rha, GalA, Glc, Gal, Ara, Fuc) with 0.6 mol/L sodium hydroxide solution, 100  $\mu$ L 0.5 mol/L PMP-methanol solutions were added and mixed. The derivatization reaction was performed at 70 °C for 100 min. Neutralize the reaction solution with the hydrochloric acid and remove residual PMP with chloroform. The prepared sample solution was filtered by a 0.22  $\mu$ m filter and analyzed by high performance liquid chromatography analyzer (1260, AGILENT, America). The ZORBAX Eclipse XDB-C18 column (4.6 mm × 250 mm, internal diam. 5  $\mu$ m) analytical column was used at 20 °C. Mobile phase A consisted of 15% acetonitrile and 85% phosphate-buffered saline, and

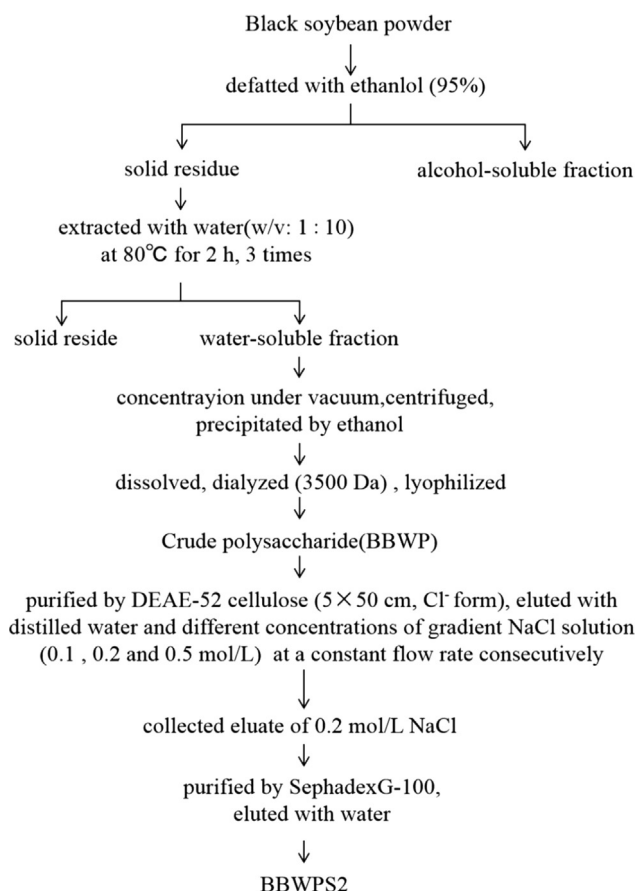


**Fig. 1** Extraction and purification scheme of the proteoglycan BBWPS2 from Black soybean.

mobile phase B consisted of 40% acetonitrile and 60% phosphate-buffered saline. The mobile phases were gradient eluted at a rate of 1 mL/min. The calibration factor was calculated by the ratio of the peak area of the standard monosaccharide, and then the ratio of the peak area of the monosaccharide in the sample was multiplied by the calibration factor to calculate the molar ratio of each monosaccharide in the sample.

### 2.7. Infrared spectra and scanning Electron microscopy analysis

Dried BBWPS2 was mixed with KBr at a volume ratio of 1:100, and pressed into thin slices for Fourier transform infrared spectrophotometer (BRUKER TENSOR 27, BRUCK, Germany) measurement between  $400\text{ cm}^{-1}$  and  $4000\text{ cm}^{-1}$  (Liu et al., 2020).

BBWPS2 dried powder sample was glued to the sample table with the conductive adhesive. After gold spraying, the surface structure of BBWPS2 was observed by scanning electron microscopy (Sun et al., 2017).

### 2.8. $\beta$ -elimination reaction and ultraviolet spectrum analysis

3 mg BBWPS2 was dissolved in distilled water or 5 mL 0.2 mol/L NaOH. After incubation at 45°C for 30 min, ultraviolet spectrum full wavelength scanning was performed (Downs et al., 1977).

### 2.9. Determination of immune activity

#### 2.9.1. Splenocyte proliferation assay

MTT (methyl thiazolyl tetrazolium) assay is a test for cell survival and growth (Kumar et al., 2018). The splenocyte proliferation assay was evaluated in vitro by the MTT method. The cells ( $1 \times 10^7/\text{mL}$ ) were incubated with different concentrations BBWPS2 (50, 100, 200  $\mu\text{g}/\text{mL}$ ) with or without ConA (5  $\mu\text{g}/\text{mL}$ ) and LPS (2.5  $\mu\text{g}/\text{mL}$ ) for 48 h. 0.5 mg/mL MTT was added and the samples were further incubated for 4 h at 37 °C. The optical density was measured at 570 nm.

#### 2.9.2. Effects of BBWPS2 on cytotoxicity and TNF- $\alpha$ production in macrophages

$1 \times 10^5/\text{mL}$  RAW264.7 cells were cultured in a 96-well plate. The cells were treated with various concentrations of BBWPS2 (50, 100, 200  $\mu\text{g}/\text{mL}$ ) or LPS (2.5 mg/mL) for 24 h. The cell culture liquid was collected for TNF- $\alpha$  production determination using the enzyme-linked immunosorbent assay (ELISA) kits (R&D) according to the instructions. The optical density was measured at 450 nm. Meanwhile, 90  $\mu\text{L}$  new culture medium and 10  $\mu\text{L}$  MTT (0.5 mg/mL) was added to the 96-well plates, and further incubated for 4 h at 37°C. After the cell culture medium was removed as much as possible, 100  $\mu\text{L}$  dimethyl sulfoxide (DMSO) was added to dissolve formazan, and the absorbance was measured at 570 nm with a microplate reader.

#### 2.9.3. Mannose receptor inhibitor assay

We determined the effect of mannose receptor inhibitor on BBWPS2 activation of RAW264.7 cells. After pretreatment with mannose solution (0.5 mg/mL) for 1 h, RAW264.7 cells were incubated with 200  $\mu\text{g}/\text{mL}$  BBWPS2 or 2.5  $\mu\text{g}/\text{mL}$  LPS for 24 h. As described in 2.9.2, the content of TNF- $\alpha$  in the culture medium was determined.

#### 2.9.4. NF- $\kappa$ B inhibitor and translocation kit assay

We tested whether BBWPS2 activated macrophages through the NF- $\kappa$ B signaling pathway using NF- $\kappa$ B inhibitor BAY 11-7082 (2  $\mu\text{mol}/\text{L}$ ). The specific experimental steps are the same as 2.9.3.

In addition, the nuclear translocation of the p65 subunit in BBWPS2-treated RAW264.7 cells was tracked by a confocal laser-scanning microscope (Leica TCS SP, LEICA, Germany). RAW264.7 cells were inoculated in 24-well plates, treated with PBS, 200  $\mu\text{g}/\text{mL}$  BBWPS2, or 2.5  $\mu\text{g}/\text{mL}$  LPS for 3 h. Then, the cells were washed, fixed and sealed for 1 h. NF- $\kappa$ B p65 antibody or secondary antibody FITC labeled goat anti-rabbit IgG (H + L) were respectively added and incubated for 1 h. After treatment with DAPI for 5 min, the blue fluorescent nucleus and green fluorescent p65 subunits were observed under the microscope.

#### 2.9.5. Real-time quantitative polymerase chain reaction

RAW264.7 cells were inoculated into 24-well plates and treated with 800  $\mu\text{g}/\text{mL}$  BBWPS2 for 6 h, then total RNA was extracted using total RNA Kit I according to the instructions. PrimeScript<sup>TM</sup> RT Master Mix was used to reverse transcribe the total RNA into cDNA, and the TB Green Premix Ex Taq<sup>TM</sup> II system was used for quantitative analysis. The reac-

tion conditions of RT-qPCR were 95 °C for 30 s, 95 °C denaturations for 5 s, 60 °C annealing for 30 s, and 40 cycles. The relative mRNA expression was calculated by the  $2^{-\Delta\Delta C_t}$  method. Actin- $\beta$  gene was used as an internal reference gene, and the RT-qPCR data were normalized. Oligonucleotide sequences of primers were designed by Primer Premier 5.0 software or determined by literature (Xia et al., 2012, Wang et al., 2019). Primer sequences were shown in Table 1.

### 2.10. Statistical analysis

Results were expressed as mean  $\pm$  standard deviation (SD). Data were analyzed by One-Way and Two-Way ANOVA with the Prism software for Windows (version 8.00; GraphPad Software).

## 3. Results

### 3.1. Preparation of Black soybean proteoglycan

We extracted protein-polysaccharide polymers through water extraction and alcohol precipitation (Fig. 1). Firstly, crude extract was isolated from Black soybean with a yield of 17.2%. Then, the proteoglycan BBWPS2 was collected with a yield of 2.1% from the crude extract by column chromatography.

### 3.2. Molecular weight and chemical compositions determination

The molecular weight is an important index to study the properties of proteoglycan (Hundschell et al., 2020). As determined by detecting the sample signal and calculating the retention time, the molecular weight of BBWPS2 was  $2.02 \times 10^5$  Da. The chemical composition results showed that the carbohydrate, protein and uronic acid contents of BBWPS2 were  $42.30 \pm 2.43\%$ ,  $22.48 \pm 1.38\%$  and  $21.78 \pm 0.63\%$ , respectively. These results showed that BBWPS2 was an acid proteoglycan.

### 3.3. Amino acids and monosaccharide composition analysis

The amino acid analysis results were shown in Table 2, BBWPS2 contained 16 kinds of amino acids, and the total content is 10.4%. It includes 8 kinds of essential amino acids (total content: 4.5%) and 8 kinds of non-essential amino acids (total content: 5.9%).

**Table 1** Primer sequences used for RT-qPCR.

Gene	Primer sequences (5'–3')
actin- $\beta$	F: TCACCCACACTGTGCCCATCTACGA; R: GGATGCCACAGGATTCCATACCCA
TNF- $\alpha$	F: ATAGCTCCCAGAAAAGCAAGC; R: CACCCCGAAGTTCAGTAGACA
TLR4	F: TCAGCAAAGTCCCTGATGACATTCC; R: AGAGGTGGTGTAAGCCATGCCA
JNK	F: ATTGAACAGCTCGGAACACC; R: GAGTCAGCTGGGAAAAGCAC
ERK	F: TGACCTCAAGCCTTCCAACC; R: ATCTGGATCTGCAACACGGG

To determine the monosaccharide composition, BBWPS2 was hydrolyzed with trifluoroacetic acid, the hydrolysates were further precolumn-derivatization with PMP for HPLC analysis (Zhang et al., 2021). As shown in Fig. 2, the monosaccharide composition analysis indicated that BBWPS2 was composed of Man, Rha, GalA, Glc, Gal, Ara and Fuc in a molar ratio of 2.35: 2.40: 24.48: 32.89: 21.13: 28.45: 1.37.

**Table 2** Amino acid content of the proteoglycan BBWPS2.

Amino acid classification	Amino acid name	Content/%
essential amino acid	Thr	0.6
	Val	0.5
	Met	0.2
	Ile	0.3
	Leu	0.7
	Phe	0.3
	His	0.8
	Lys	1.1
nonessential amino acid	Asp	1.2
	Ser	0.8
	Glu	1.5
	Gly	0.5
	Tyr	0.2
	Arg	0.5
	Ala	0.7
	Pro	0.5
Cys	0.0	

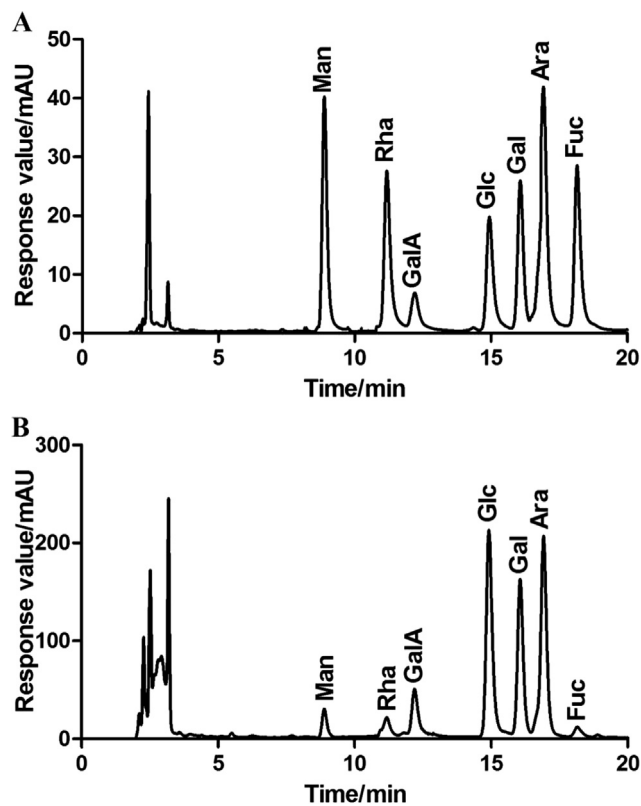


**Fig. 2** The monosaccharide compositions of mixed monosaccharide standards (A) and BBWPS2 (B).

### 3.4. IR and ultraviolet spectrum analysis

As shown in Fig. 3A, there was a wide absorption peak at  $3401.12\text{ cm}^{-1}$ , indicating that the structure of BBWPS2 contained hydroxyl functional groups. Combined with the chemical composition analysis, the absorption peak of  $\text{C}=\text{O}$  stretching vibration near  $1654\text{ cm}^{-1}$  may be caused by the stretching vibration of the amide bond in the protein structure, and it may also be caused by the  $\text{C}=\text{O}$  bond in the uronic acid structure. The absorption peaks between  $950\text{ cm}^{-1}$  and  $1200\text{ cm}^{-1}$  were caused by the stretching vibration of C-O-C and C-O (Biao et al., 2020).

Under alkaline conditions, the *O*-glycosidic bond undergoes the  $\beta$ -removal reaction, and the absorbance value at 240 nm increased significantly, while the *N*-glycosidic bond does not undergo the  $\beta$ -elimination reaction (Kishimoto et al., 1999). The ultraviolet scanning result of BBWPS2 was shown in Fig. 3B. After NaOH treatment, the absorbance value at 240 nm increased obviously, and the spectral shape changed. It indicated that the glycosidic bond type of BBWPS2 was *O*-type.

In addition, the SEM images of BBWPS2 at 800-fold and 2000-fold were presented in Fig. 3C, 3D. As observed, BBWPS2 had a smooth surface and has irregular lamellar structure. It may indicate powerful intermolecular forces in BBWPS2.

### 3.5. BBWPS2 promoted splenocyte proliferation

Splenic lymphocytes are transformed from stationary lymphocytes to lymphoblastic cells by mitogen stimulation, resulting in mitosis. Therefore, splenocyte proliferation is an important indicator of immune cell level. Mitogen ConA and LPS stimulate T and B cell proliferation, respectively. (Chen et al., 2003). As shown in Fig. 4A, BBWPS2 had the potential to promote

the proliferation of splenic lymphocytes. BBWPS2 also promoted LPS-stimulated B cells proliferation and ConA-stimulated T cells proliferation in a concentration-dependent manner (Fig. 4B, 4C). The results indicated that BBWPS2 promoted the proliferation of T/B cells.

### 3.6. BBWPS2 promoted TNF- $\alpha$ production

MTT assay showed that BBWPS2 had no cell cytotoxicity to RAW264.7 macrophages at different concentrations (Fig. 5A). TNF- $\alpha$  is a kind of small molecular peptide synthesized and excreted by immune cells, which plays an important role in immune regulation (Liu et al., 2017). Here, we measured the secretion amount of TNF- $\alpha$  to determine whether BBWPS2 could activate macrophages. Our results found that BBWPS2 promoted the production of TNF- $\alpha$  and significantly increased the accumulation of TNF- $\alpha$  ( $p < 0.01$ ). There was a positive correlation between TNF- $\alpha$  production and BBWPS2 concentration (Fig. 5B). The result indicated that BBWPS2 significantly activated the immune response of macrophages.

### 3.7. BBWPS2 activated macrophages via the mannose receptor

The mannose receptors (MR) are antigenic proteins on the surface of macrophages that recognize and bind mannose or fucose residues to activate macrophages (Gordon 2002). Based on the monosaccharide composition analysis results, BBWPS2 contained mannose and fucose. Thus, we used mannose inhibitors to detect whether BBWPS2 activated macrophages through mannose receptors. As expected, mannose inhibitors have no impact on the control group and the LPS-treated group ( $p > 0.05$ ), but the TNF- $\alpha$  content in the culture supernatant was significantly decreased in the BBWPS2-treated group ( $p < 0.001$ ) (Fig. 5C). These data suggested that

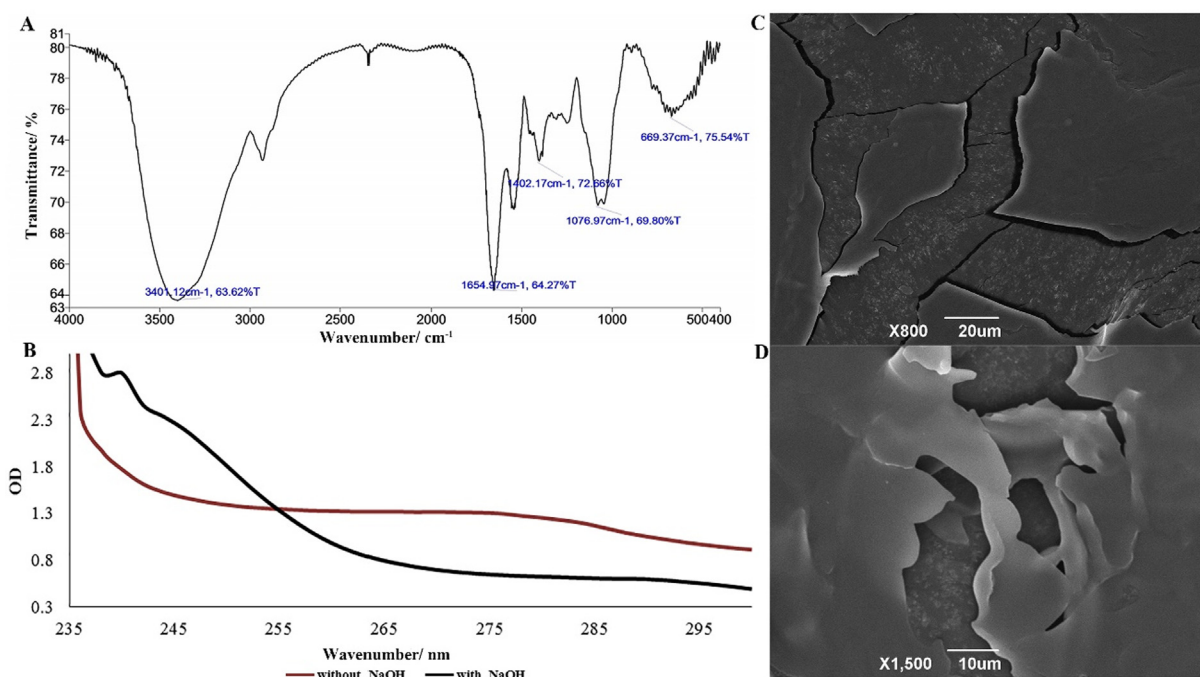
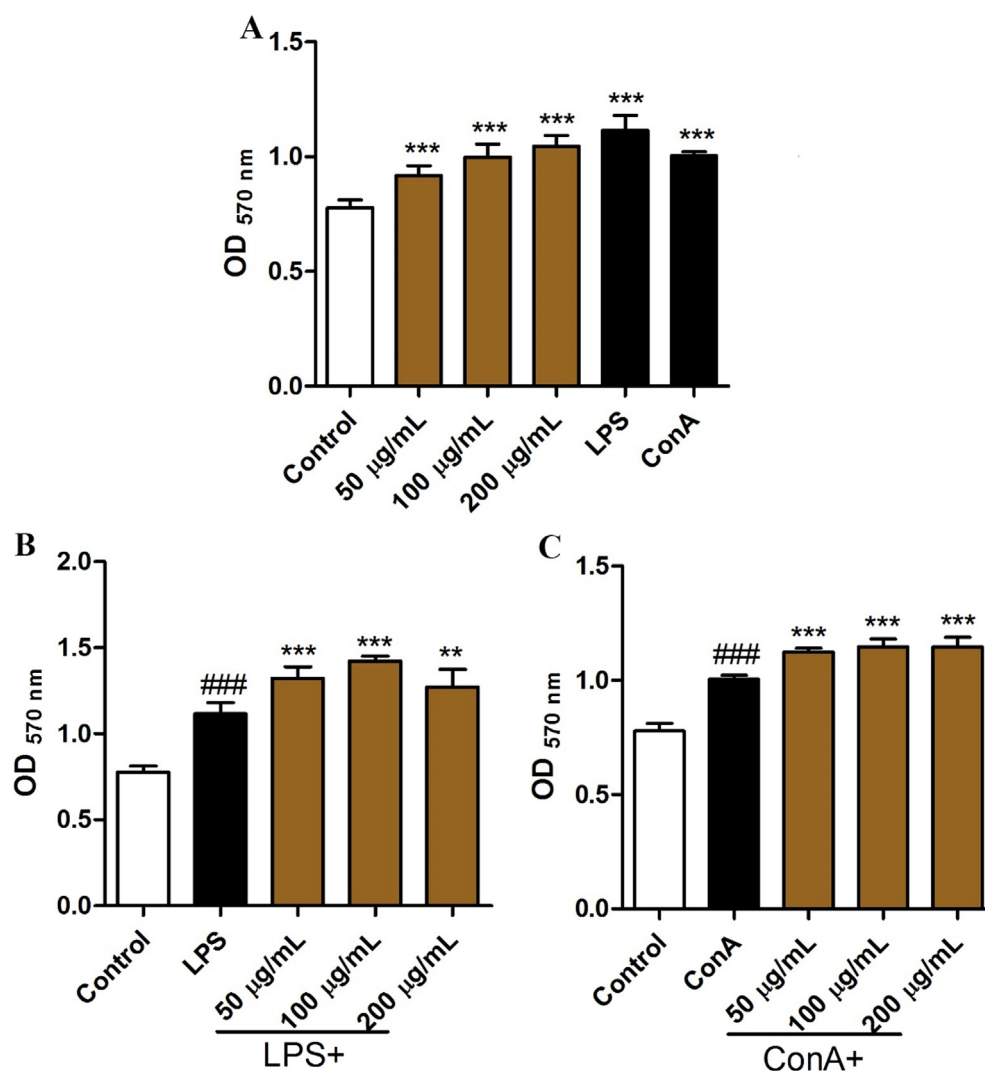


Fig. 3 Infrared spectra (A), Uv scan (B) and Electron microscopy images (C, D) of BBWPS2.



**Fig. 4** Effects of BBWPS2 on the splenocyte proliferation. The mice spleen cells were incubated with BBWPS2 at different concentrations (50, 100, 200  $\mu\text{g/mL}$ ) alone (A), in the presence of mitogens ConA (5  $\mu\text{g/mL}$ ) (B) or LPS (2.5  $\mu\text{g/mL}$ ) (C) for 48 h. MTT was added and incubated. The optical density was measured. Data shown were mean  $\pm$  SD of 3 independent experiments. (###)  $p < 0.001$  compared with the control group, (\*\*\*)  $p < 0.001$ , (\*\*)  $p < 0.01$ , and (\*)  $p < 0.05$  compared with the control (A), LPS (B) or ConA (C) group.

BBWPS2 activated RAW264.7 cells through the MR-mediated signaling pathway to promote TNF- $\alpha$  secretion.

### 3.8. BBWPS2 activated macrophages via the NF- $\kappa$ B signaling pathway

The NF- $\kappa$ B signaling pathway is one of the classical pathways in macrophage activation by exogenous antigens. NF- $\kappa$ B, a “fast-acting” primary transcription factor, is an important hub of this pathway (Dresselhaus and Meffert 2019). LPS stimulates macrophages to release cytokines through NF- $\kappa$ B. BAY 11-7082 is a specific inhibitor of NF- $\kappa$ B. As shown in Fig. 5C, BAY 11-7082 did not affect the control group ( $p > 0.05$ ), and TNF- $\alpha$  contents in the culture supernatant of the BBWPS2-treated group and the LPS-treated group were significantly decreased ( $p < 0.001$ ). These results indicated that BBWPS2 could promote the production of TNF- $\alpha$  by activating the nuclear transcription factor NF- $\kappa$ B in RAW264.7 cells.

To further demonstrate whether BBWPS2 could activate NF- $\kappa$ B, we used the immune fluorescence labeling to trace the translocation of the p65 subunit (Kim et al., 2019). After LPS or BBWPS2-treated RAW264.7 cells, the p65 subunit (green fluorescence) in RAW264.7 cells was translocated to the nucleus (blue fluorescence) under the fluorescence microscope (Fig. 6). Thus, it further confirmed that the NF- $\kappa$ B signaling pathway was involved in the BBWPS2-induced activation of RAW264.7 cells. These results indicated that BBWPS2 was an effective NF- $\kappa$ B activator and could participate in the inflammatory response and immune response of cells.

### 3.9. BBWPS2 activated macrophages via the MAPK signaling pathway

As shown in Fig. 7, compared with the control group, the TNF- $\alpha$  was significantly up-regulated after BBWPS2 treatment ( $p < 0.001$ ). The RT-qPCR results also indicated that

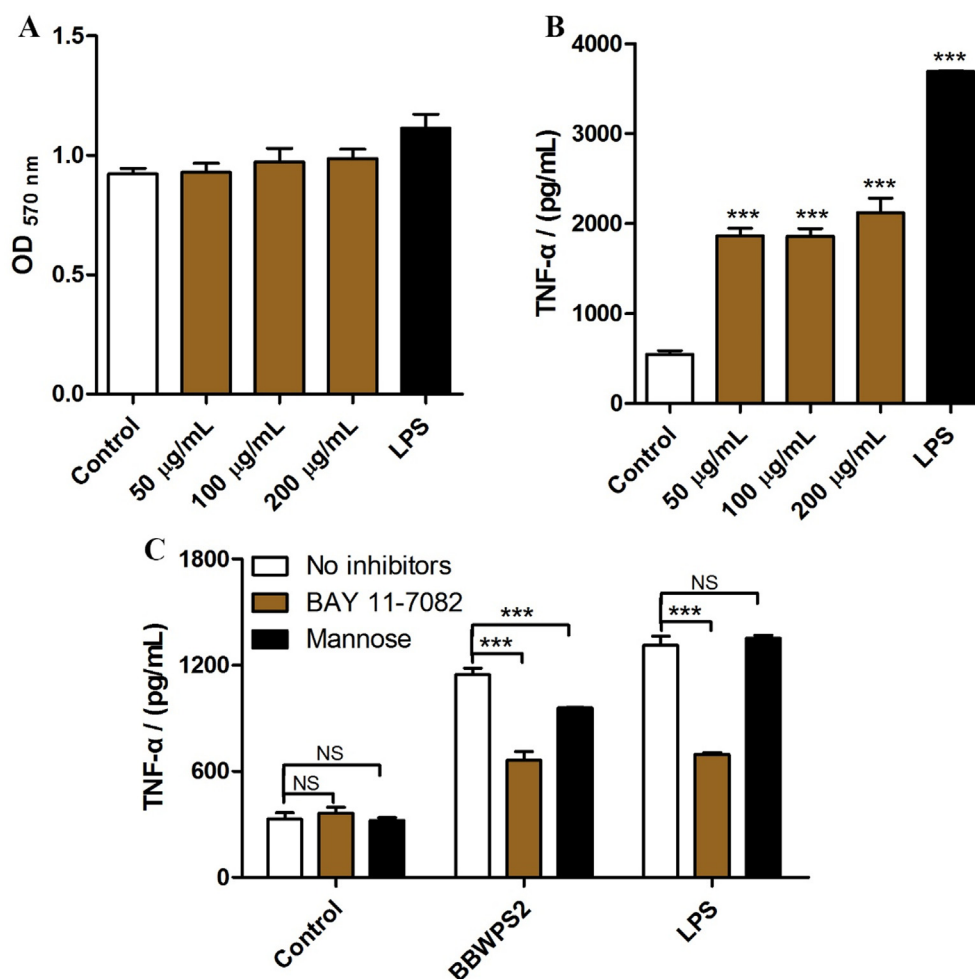


**Fig. 5** Effects of BBWPS2 on the secretion of TNF- $\alpha$  in RAW264.7 cells. (A, B) RAW264.7 cells were treated with BBWPS2 or LPS for 24 h. (C) RAW264.7 cells were pretreated with BAY 11-7082 (2  $\mu$ mol/L) or mannose (500  $\mu$ g/mL) for 1 h before incubation with 200  $\mu$ g/mL BBWPS2 or 2.5  $\mu$ g/mL LPS for 24 h. The content of TNF- $\alpha$  in the culture medium was determined by ELISA kit.

BBWPS2 can activate TNF- $\alpha$  mRNA expression level of macrophages. The mitogen-activated protein kinase (MAPK) signaling pathway is the core pathway of cell exogenous signal transmission, and the c-Jun N-terminal kinase (JNK) and the extracellular regulated protein kinases (ERK) signaling pathways are the main branch routes of the MAPK signaling pathway that are responsible for cell inflammation, growth and differentiation, and JNK and ERK are the key factors in these two branch routes (Ko et al., 2019). Compared with the control group, JNK and ERK genes were significantly upregulated ( $p < 0.05$ ). These results suggest that BBWPS2 may also activate macrophages through MAPK signaling to trigger cellular immune responses.

#### 4. Discussion

In the present work, we identified a novel proteoglycan with immunomodulatory activity from Black soybean. The structural analysis displayed that BBWPS2 is a proteoglycan linked by an *O*-glycosidic bond, containing various monosaccharides, amino acids and  $21.78 \pm 0.63\%$  uronic acid. The immunolog-

ical activity analysis indicated BBWPS2 significantly promotes splenocyte proliferation and activates macrophages to secrete cellular messengers TNF- $\alpha$ .

Moreover, we try to confirm the underlying molecular actions of BBWPS2 for enhancing the immune system. It has been known that bioactivities of protein-polysaccharide are closely related to their chemical structures such as compositional monosaccharides and amino acids, types of chemical linkages, and molecular weight distributions (Tabarsa et al., 2015, Kelly and Pearce 2020). Exogenous protein-polysaccharide polymers usually activate macrophages through receptor-mediated activation, which in turn triggers a cascade of signals within the cell to initiate an immune response (Zong et al., 2012, Han et al., 2018). The results of monosaccharide composition showed that BBWPS2 contained mannose and fucose. These two monosaccharides are classical ligands for the mannose receptor, which is the surface recognition receptors of macrophages, participates in antigen presentation and acquired immune response and play an important role in natural immune defense against pathogen infection (Taylor et al., 2005, Liu et al., 2008). Here, the mannose

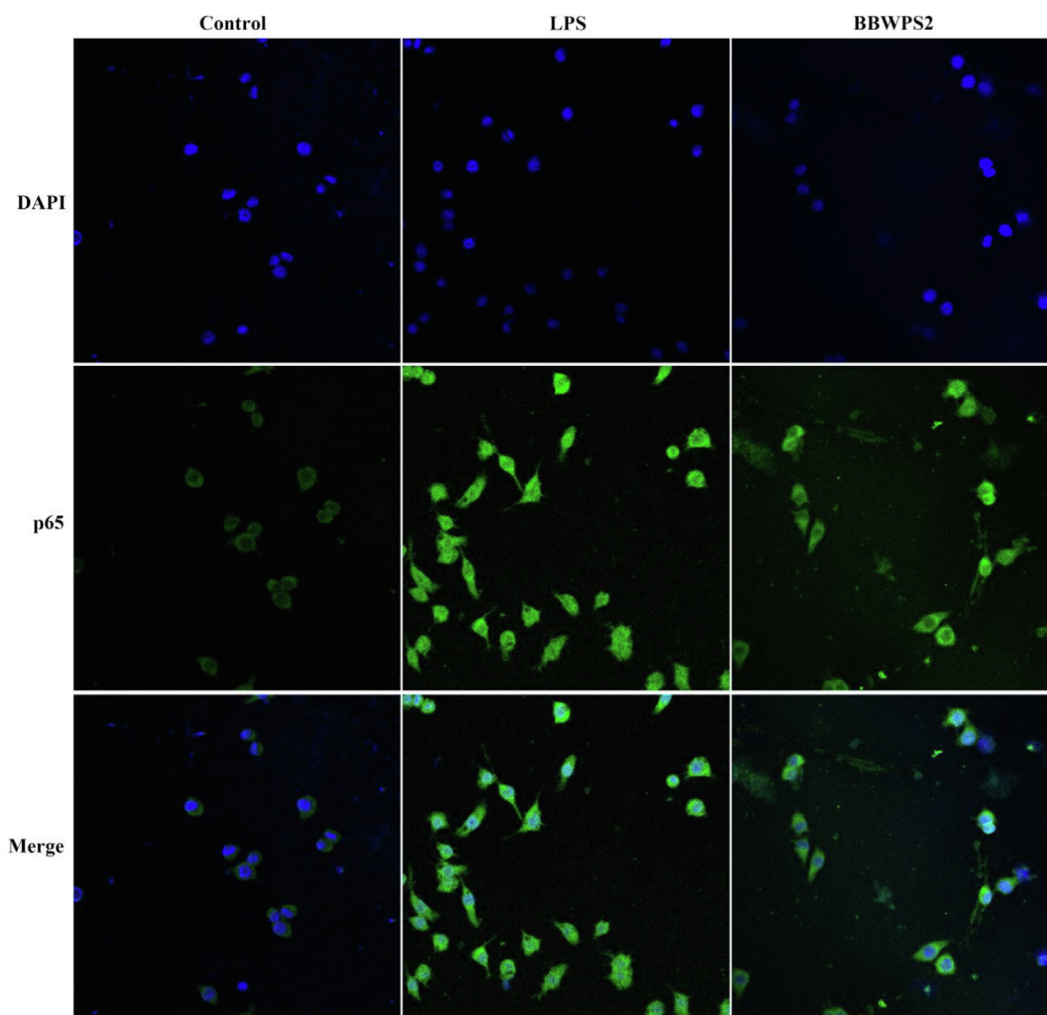


**Fig. 6** BBWPS2 activated the NF- $\kappa$ B signaling in RAW264.7 cells. RAW264.7 cells were treated with BBWPS2 (200  $\mu$ g/mL) or LPS (2.5  $\mu$ g/mL) for 3 h. p65 subunit translocated into nuclei (DAPI) was obtained by confocal laser microscopy.

receptor-specific inhibitor block assay showed that BBWPS2 can recognize and bind to mannose receptors and activate

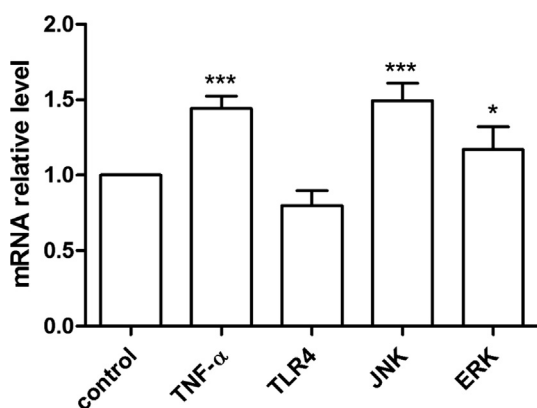


**Fig. 7** The effects of BBWPS2 on the mRNA expression level of pathway-related genes in RAW264.7 cell. The expression of genes was investigated after treatment with BBWPS2 for 6 h. Compared to the control group, (\*\*\*)  $p < 0.001$ , (\*)  $p < 0.05$ .

macrophage. However, surface receptor binding is only the first step in macrophage activation. Cell surface signals are transmitted into the cell and trigger intracellular signaling pathways that activate macrophages to produce an immune response (Yang et al., 2019; Feng et al., 2021). NF- $\kappa$ B specific inhibitor blocking assay and p65 protein subunit translocation observation showed that BBWPS2 could regulate macrophage immune response by activating NF- $\kappa$ B (Fig. 5 and Fig. 6). In addition, the RT-qPCR assay revealed that BBWPS2 also triggered macrophage immune response via the MAPK signaling pathway (Fig. 7). In brief, BBWPS2 was recognized by mannose receptors of macrophage surface, further triggering NF- $\kappa$ B/MAPK signaling pathway to regulate macrophage immune response and induce macrophages to secrete TNF- $\alpha$ .

In addition, it can be seen from Fig. 2 that mannose and fructose in the sample are minor components, while other sugars are dominant in the sample. We suspect that other receptors may be involved in BBWPS2 activating macrophage immune responses. Therefore, the immune activity and related molecular mechanism of BBWPS2 will be further explored in animal models in the next stage.

## 5. Conclusion

In summary, a novel acid proteoglycan BBWPS2 with the molecular weight of  $2.02 \times 10^5$  Da was successfully isolated from the water extract of the Black soybean. Its immune activity and the underlying mechanism were explored. Our data demonstrated that BBWPS2 promoted splenocyte proliferation, and activated macrophages through the classical MR-mediated NF- $\kappa$ B/MAPK signaling pathway. Thus, the current study demonstrates that BBWPS2 has the potential for becoming a novel natural immunopotentiator and also provides strong evidence for the immunomodulatory activity of Black soybean proteoglycan.

## Declaration of Competing Interest

The authors declare that they have no known competing financial interests or personal relationships that could have appeared to influence the work reported in this paper.

## Acknowledgements

This work was supported by the National Natural Science Foundation of China (No.31800678), The National Key Research and Development Program of China (2021YFD1600601-2), Science and Technology Innovation Project of Colleges and Universities in Shanxi Province (No. 2021L146), Key Research and Development Project Key Program of Shanxi Province (201903D211006-1), and Breeding Project of Shanxi Agricultural University (YZGC096).

## References

- Barba, C., Alonso, C., Sánchez, I., et al, 2017. Soybean-fragmented proteoglycans against skin aging. *J. Cosmet. Laser Therapy: Official Publ. Eur. Soc. Laser Dermatol.* 19, 237–244. <https://doi.org/10.1080/14764172.2017.1288259>.
- Biao, Y., Jiannan, H., Yaolan, C., et al, 2020. Identification and characterization of antioxidant and immune-stimulatory polysaccharides in flaxseed hull. *Food Chem.* 315, <https://doi.org/10.1016/j.foodchem.2020.126266> 126266.
- Blumenkrantz, N., Asboe-Hansen, G., 1973. New method for quantitative determination of uronic acids. *Anal. Biochem.* 54, 484–489.
- Chen, H.L., Li, D.F., Chang, B.Y., et al, 2003. Effects of lentinan on broiler splenocyte proliferation, interleukin-2 production, and signal transduction. *Poult. Sci.* 82, 760–766. <https://doi.org/10.1093/ps/82.5.760>.
- Downs, F., Peterson, C., Murty, V.L., et al, 1977. Quantitation of the beta-elimination reaction as used on glycoproteins. *Int. J. Pept. Protein Res.* 10, 315–322. <https://doi.org/10.1111/j.1399-3011.1977.tb02803.x>.
- Dresselhaus, E.C., Meffert, M.K., 2019. Cellular Specificity of NF- $\kappa$ B Function in the Nervous System. *Front. Immunol.* 10, 1043. <https://doi.org/10.3389/fimmu.2019.01043>.
- Feng, S., Ding, H., Liu, L., et al, 2021. Astragalus polysaccharide enhances the immune function of RAW264.7 macrophages via the NF- $\kappa$ B p65/MAPK signaling pathway. *Exp. Therapeut. Med.* 21, 20. <https://doi.org/10.3892/etm.2020.9452>.
- Gordon, S., 2002. Pattern recognition receptors: doubling up for the innate immune response. *Cell* 111, 927–930. [https://doi.org/10.1016/s0092-8674\(02\)01201-1](https://doi.org/10.1016/s0092-8674(02)01201-1).
- Han, C., Yang, J., Song, P., et al, 2018. Effects of *Salvia miltiorrhiza* Polysaccharides on Lipopolysaccharide-Induced Inflammatory Factor Release in RAW264.7 Cells. *J. Interferon Cytokine Res.: Official J. Int. Soc. Interferon Cytokine Res.* 38, 29–37. <https://doi.org/10.1089/jir.2017.0087>.
- Hayat, I., Ahmad, A., Masud, T., et al, 2014. Nutritional and health perspectives of beans (*Phaseolus vulgaris* L.): an overview. *Crit. Rev. Food Sci. Nutr.* 54, 580–592. <https://doi.org/10.1080/10408398.2011.596639>.
- Hayes, M., 2020. Measuring Protein Content in Food: An Overview of Methods. *Foods* (Basel, Switzerland). 9. <https://doi.org/10.3390/foods9101340>.
- Honda, S., Akao, E., Suzuki, S., et al, 1989. High-performance liquid chromatography of reducing carbohydrates as strongly ultraviolet-absorbing and electrochemically sensitive 1-phenyl-3-methyl-5-pyrazolone derivatives. *Anal. Biochem.* 180, 351–357.
- Hsieh-Lo, M., Castillo-Herrera, G., 2020. Black Bean Anthocyanin-Rich Extract from Supercritical and Pressurized Extraction Increased In Vitro Antidiabetic Potential. While Having Similar Storage Stabil. 9. <https://doi.org/10.3390/foods9050655>.
- Hundscheil, C.S., Jakob, F., Wagemans, A.M., 2020. Molecular weight dependent structure of the exopolysaccharide levan. *Int. J. Biol. Macromol.* 161, 398–405. <https://doi.org/10.1016/j.ijbiomac.2020.06.019>.
- Jakab, L., 2016. Biological role of heterogeneous glycoprotein structures. *Orv. Hetil.* 157, 1185–1192. <https://doi.org/10.1556/650.2016.30436>.
- Kelly, B., Pearce, E.L., 2020. Amino Assets: How Amino Acids Support Immunity. *Cell Metab.* 32, 154–175. <https://doi.org/10.1016/j.cmet.2020.06.010>.
- Kim, G.Y., Park, S.K., Lee, M.K., et al, 2003. Proteoglycan isolated from *Phellinus linteus* activates murine B lymphocytes via protein kinase C and protein tyrosine kinase. *Int. Immunopharmacol.* 3, 1281–1292. [https://doi.org/10.1016/s1567-5769\(03\)00115-2](https://doi.org/10.1016/s1567-5769(03)00115-2).
- Kim, H.W., Shin, M.S., Lee, S.J., et al, 2019. Signaling pathways associated with macrophage-activating polysaccharides purified from fermented barley. *Int. J. Biol. Macromol.* 131, 1084–1091. <https://doi.org/10.1016/j.ijbiomac.2019.03.159>.
- Kishimoto, T., Watanabe, M., Mitsui, T., et al, 1999. Glutelin basic subunits have a mammalian mucin-type O-linked disaccharide side chain. *Arch. Biochem. Biophys.* 370, 271–277. <https://doi.org/10.1006/abbi.1999.1406>.
- Ko, W., Quang, T.H., Sohn, J.H., 2019. Anti-inflammatory effect of 3,7-dimethyl-1,8-hydroxy-6-methoxyisochroman via nuclear factor erythroid 2-like 2-mediated heme oxygenase-1 expression in lipopolysaccharide-stimulated RAW264.7 and BV2. *Cells* 41, 337–348. <https://doi.org/10.1080/08923973.2019.1608559>.
- Kumar, P., Nagarajan, A., Uchil, P.D., 2018. Analysis of Cell Viability by the MTT Assay. *Cold Spring Harbor protocols.* 2018. <https://doi.org/10.1101/pdb.prot095505>.
- Liu, L., Guo, Z., Lv, Z., et al, 2008. The beneficial effect of Rheum tanguticum polysaccharide on protecting against diarrhea, colonic inflammation and ulceration in rats with TNBS-induced colitis: the role of macrophage mannose receptor in inflammation and immune response. *Int. Immunopharmacol.* 8, 1481–1492. <https://doi.org/10.1016/j.intimp.2008.04.013>.
- Liu, L.L., Wang, L., Zonderman, J., et al, 2020. Automated, High-Throughput Infrared Spectroscopy for Secondary Structure Analysis of Protein Biopharmaceuticals. *J. Pharm. Sci.* 109, 3223–3230. <https://doi.org/10.1016/j.xphs.2020.07.030>.
- Liu, X., Xie, J., Jia, S., et al, 2017. Immunomodulatory effects of an acetylated *Cyclocarya paliurus* polysaccharide on murine macrophages RAW264.7. *Int. J. Biol. Macromol.* 98, 576–581. <https://doi.org/10.1016/j.ijbiomac.2017.02.028>.
- Reverri, E.J., Randolph, J.M., Steinberg, F.M., et al, 2015. Black Beans, Fiber, and Antioxidant Capacity Pilot Study: Examination of Whole Foods vs. Functional Components on Postprandial Metabolic, Oxidative Stress, and Inflammation in Adults with Metabolic Syndrome. *Nutrients.* 7, 6139–6154. <https://doi.org/10.3390/nu7085273>.
- Sun, Q., Sun, Y., Juzenas, K., 2017. Immunogold scanning electron microscopy can reveal the polysaccharide architecture of xylem cell

- walls. *J. Exp. Bot.* 68, 2231–2244. <https://doi.org/10.1093/jxb/erx103>.
- Tabarsa, M., Park, G.-M., Shin, I.-S., et al, 2015. Structure-Activity Relationships of Sulfated Glycoproteins from *Codium fragile* on Nitric Oxide Releasing Capacity from RAW264.7 Cells. *Mar. Biotechnol.* 17, 266–276. <https://doi.org/10.1007/s10126-015-9615-2>.
- Taylor, P.R., Gordon, S., Martinez-Pomares, L., 2005. The mannose receptor: linking homeostasis and immunity through sugar recognition. *Trends Immunol.* 26, 104–110. <https://doi.org/10.1016/j.it.2004.12.001>.
- Wang, J., Wang, H., Zhang, H., et al, 2019. Immunomodulation of ADPs-1a and ADPs-3a on RAW264.7 cells through NF- $\kappa$ B/ MAPK signaling pathway. *Int. J. Biol. Macromol.* 132, 1024–1030. <https://doi.org/10.1016/j.ijbiomac.2019.04.031>.
- Xia, M.Z., Liang, Y.L., Wang, H., et al, 2012. Melatonin modulates TLR4-mediated inflammatory genes through MyD88- and TRIF-dependent signaling pathways in lipopolysaccharide-stimulated RAW264.7 cells. *J. Pineal Res.* 53, 325–334. <https://doi.org/10.1111/j.1600-079X.2012.01002.x>.
- Yang, A., Fan, H., Zhao, Y., et al, 2019. An immune-stimulating proteoglycan from the medicinal mushroom *Huaier* up-regulates NF- $\kappa$ B and MAPK signaling via Toll-like receptor 4. *J. Biol. Chem.* 294, 2628–2641. <https://doi.org/10.1074/jbc.RA118.005477>.
- Zeng, Y., Cai, W., Shao, X., 2015. Quantitative analysis of 17 amino acids in tobacco leaves using an amino acid analyzer and chemometric resolution. *J. Sep. Sci.* 38, 2053–2058. <https://doi.org/10.1002/jssc.201500090>.
- Zhang, W., Song, D., Xu, D., et al, 2015a. Characterization of polysaccharides with antioxidant and immunological activities from *Rhizoma Acori Tatarinowii*. *Carbohydr. Polym.* 133, 154–162. <https://doi.org/10.1016/j.carbpol.2015.07.018>.
- Zhang, W., Sun, F., Niu, H., et al, 2015b. Mechanistic insights into cellular immunity of chondroitin sulfate A and its zwitterionic N-deacetylated derivatives. *Carbohydr. Polym.* 123, 331–338. <https://doi.org/10.1016/j.carbpol.2015.01.059>.
- Zhang, W.H., Wu, J., Weng, L., et al, 2020. An improved phenol-sulfuric acid method for the determination of carbohydrates in the presence of persulfate. *Carbohydr. Polym.* 227,. <https://doi.org/10.1016/j.carbpol.2019.115332> 115332.
- Zhang, X.X., Li, J.Q., Li, M.S., et al, 2021. Isolation, structure identification and hepatoprotective activity of a polysaccharide from *Sabia parviflora*. *Bioorg. Med. Chem. Lett.* 32,. <https://doi.org/10.1016/j.bmcl.2020.127719> 127719.
- Zong, A., Cao, H., Wang, F., 2012. Anticancer polysaccharides from natural resources: a review of recent research. *Carbohydr. Polym.* 90, 1395–1410. <https://doi.org/10.1016/j.carbpol.2012.07.026>.